Applied Surface Science 371 (2016) 583–589

Contents lists available at ScienceDirect

Applied Surface Science

journal homepage: www.elsevier.com/locate/apsusc

Laser textured surface gradients

Van Duong Ta[a,*], Andrew Dunn[a], Thomas J. Wasley[b], Ji Li[b], Robert W. Kay[b], Jonathan Stringer[c], Patrick J. Smith[c], Emre Esenturk[d], Colm Connaughton[d,e], Jonathan D. Shephard[a]

[a] Institute of Photonics and Quantum Sciences, Heriot-Watt University, Edinburgh EH14 4AS, UK
[b] Additive Manufacturing Research Group, Loughborough University, Leicestershire LE11 3TU, UK
[c] Laboratory of Applied Inkjet Printing, Department of Mechanical Engineering, University of Sheffield, Sheffield S1 4BJ, UK
[d] Warwick Mathematics Institute, Zeeman Building, University of Warwick, Coventry CV4 7AL, UK
[e] Centre for Complexity Science, Zeeman Building, University of Warwick, Coventry CV4 7AL, UK

ARTICLE INFO

Article history:
Received 11 January 2016
Received in revised form 3 March 2016
Accepted 5 March 2016
Available online 9 March 2016

Keywords:
Roughness gradients
Wettability gradients
Laser surface texturing
Nanosecond laser
Chemical sensors

ABSTRACT

This work demonstrates a novel technique for fabricating surfaces with roughness and wettability gradients and their subsequent applications for chemical sensors. Surface roughness gradients on brass sheets are obtained directly by nanosecond laser texturing. When these structured surfaces are exposed to air, their wettability decreases with time (up to 20 days) achieving both spatial and temporal wettability gradients. The surfaces are responsive to organic solvents. Contact angles of a series of dilute isopropanol solutions decay exponentially with concentration. In particular, a fall of 132° in contact angle is observed on a surface gradient, one order of magnitude higher than the 14° observed for the unprocessed surface, when the isopropanol concentration increased from 0 to 15.6 wt%. As the wettability changes gradually over the surface, contact angle also changes correspondingly. This effect offers multi-sensitivity at different zones on the surface and is useful for accurate measurement of chemical concentration.

1. Introduction

Surfaces with special properties including superhydrophobicity, superhydrophilicity and gradient are important for numerous applications in biomedical, microfluidics, sensors and suppression of the coffee-stain effect [1–6]. While super-hydrophobic/-hydrophilic surfaces exhibit either incomplete or complete wetting, surfaces with wettability gradients are more interesting because their wettability changes gradually over their length in space and may even develop in time [5]. Surface gradients are common in nature which demonstrate unique abilities such as directional water collection (from humid air or fog) [7,8]. Artificial gradients have also been fabricated with potential in controlling liquid movement, solving heat transfer problems and, pH sensitive devices [9–12].

Gradients can be simply classified into two categories where surfaces possess either a gradual variation of chemical or physical properties [5]. Physical gradients have gradual patterns or roughness processed on the surface [13–17]. Chemical gradients are more common, which are primarily formed by coating or depositing thin chemical layers on original material [9–12,18–24].

Recently, laser texturing has been demonstrated as an excellent tool for modifying surface roughness on nearly all types of materials [25–29]. Compared with chemical methods, direct laser texturing is a low waste, single-step procedure with potentially high processing rate and importantly, the ability to control surface roughness or wettability directly on the original materials without coating [30–32]. However, directly laser texturing these surface gradients have been rarely studied with a few reports that involve laser textured groove structures with a regular change in groove spacing [33,34]. As a result, investigation of direct laser patterning structure gradients (both spatially and temporally) using novel approaches is necessary and significant for taking advantage of laser technology for the creation of smart surfaces.

This work demonstrates surface gradients obtained by direct nanosecond laser texturing and their applications as multi-sensitivity chemical sensors.

* Corresponding author.
E-mail address: d.ta@hw.ac.uk (V.D. Ta).

http://dx.doi.org/10.1016/j.apsusc.2016.03.054

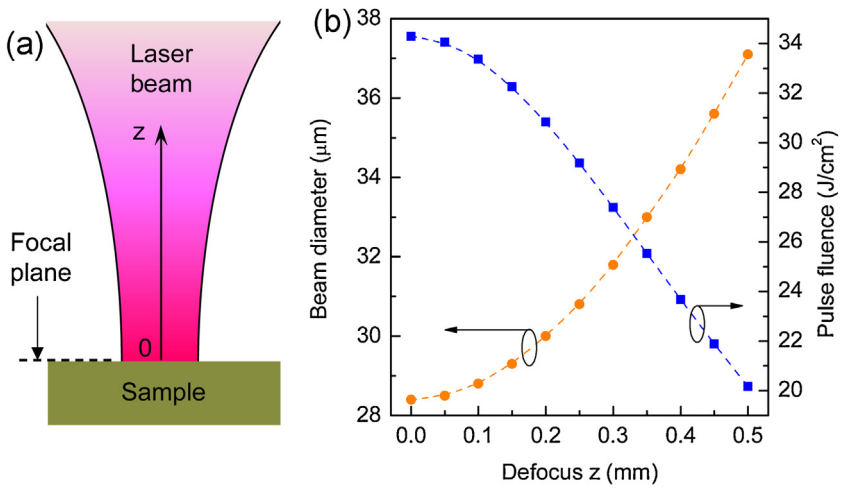

Fig. 1. Characteristics of focused laser beam used for surface texturing. (a) Schematic of the beam shape during fabrication process. (b) Calculated beam diameter determined as $1/e^2$ of maximum intensity profile and the corresponding pulse fluence as function of the defocus distance z.

2. Materials and methods

2.1. Materials

All laser processing was performed on 0.6 mm thick brass sheets (CZ121M, RS Components). The samples were cleaned with isopropanol before irradiating with laser.

2.2. Laser surface texturing

The surface morphology of the samples was modified by a nanosecond pulsed fibre laser (SPI, 20W EP-S) with a wavelength of 1064 nm, pulse duration of ~220 ns and repetition rate of 25 kHz. The fibre laser output is collimated before delivery to a galvanometer scanner and F-Theta focusing lens. The laser beam is scanned across the sample surface with a nominal focal spot size of 28.4 μm. Parallel micro-groove structures with a fixed hatch (scan line separation h) distance between them were textured. The scanning speed of 75 mm/s and the laser pulse energy of 0.252 mJ was fixed for all fabrication processes.

2.3. Surface characterization

The surface morphology of the laser textured samples was studied by means of scanning electron microscope (SEM) and optical microscope (Leica DM6000M). The arithmetic average of surface roughness (R_s) was obtained from z data measured with the Leica microscope on an area of ~1 mm^2.

Surface wettability was characterized by contact angle (θ) of ~5 μL deionized water droplets deposited on top of the samples. The contact angle was determined by analyzing droplet images (captured by a Unibrain 1394 camera) using the software FTA32 (version 2.0).

2.4. Preparation of isopropanol solution and sensing demonstration

Several isopropanol solutions with percent compositions (mass of solute/total mass of solution) up to 15.6 wt% were made by mixing various amounts of isopropanol (99.5% purity) in deionized water. Isopropanol solution droplets (~5 μL) on gradient surfaces were captured and their contact angles were determined as described in Section 2.3.

3. Results and discussion

3.1. Characteristics of focused laser beam

For laser processing, the laser beam is generally focused on the sample surface during fabrication to optimize light-matter interaction (Fig. 1a). The beam spot can be characterized by a defocus distance (z) where a positive value indicates that the beam focus is above the surface. Fig. 1b plots calculated pulse fluences versus z. It can be seen that at the focal plane (z = 0 mm), the fluence is the highest, about 34 mJ/cm^2, corresponding to the smallest beam diameter of 28.4 μm. The fluence reduces with increasing z and when z = 0.5 mm (a beam size of 37.1 μm), it drops to 20 mJ/cm^2, about 59% of the original value. As the morphology of laser textured surface strongly relates to laser power, the gradual change of laser fluence with z opens up the possibility of creating surface gradients by direct laser writing. It is demonstrated that by tilting the sample (discussed later) laser texturing surface gradients can be fabricated.

3.2. Effect of laser radiation on surface morphology

Fig. 2a shows schematic of direct laser writing parallel microgrooves on the brass surface using the scan head. The effect of laser radiation on surface morphology depends on the value of h and sample's position relative to focal point. For fixed h, the effect is the greatest when the processing surface is at the focal plane (z = 0 mm). As shown in Fig. 2b, the textured sample exhibits a dark colour due to a combination of oxide formation and non-reflecting properties caused by increased roughness. In contrast, for z = 0.45 mm (Fig. 2c), the fabricated surface shows a much lighter colour which indicates that the surface has less oxide and a lower roughness. Surface roughness measurements were performed on these samples and the average R_s was found to be ~2.6 μm for z = 0 mm, which is two times higher than that of 1.3 μm for z = 0.45 mm. The result confirms that laser induced roughness can be controlled by adjusting sample position vertically to laser beam direction. To get better understanding of surface morphology, SEM analysis was carried out and is shown in Fig. 3. The result indicates clear differences between the two cases. For z = 0 mm, corresponding to a fluence of 34.3 mJ/cm^2, a large amount of material was evaporated which created significant debris and formed obvious microgrooves. In contrast, for z = 0.45 mm the line structures were not completely formed as the laser fluence of 21.9 mJ/cm^2 is close to the ablation threshold.

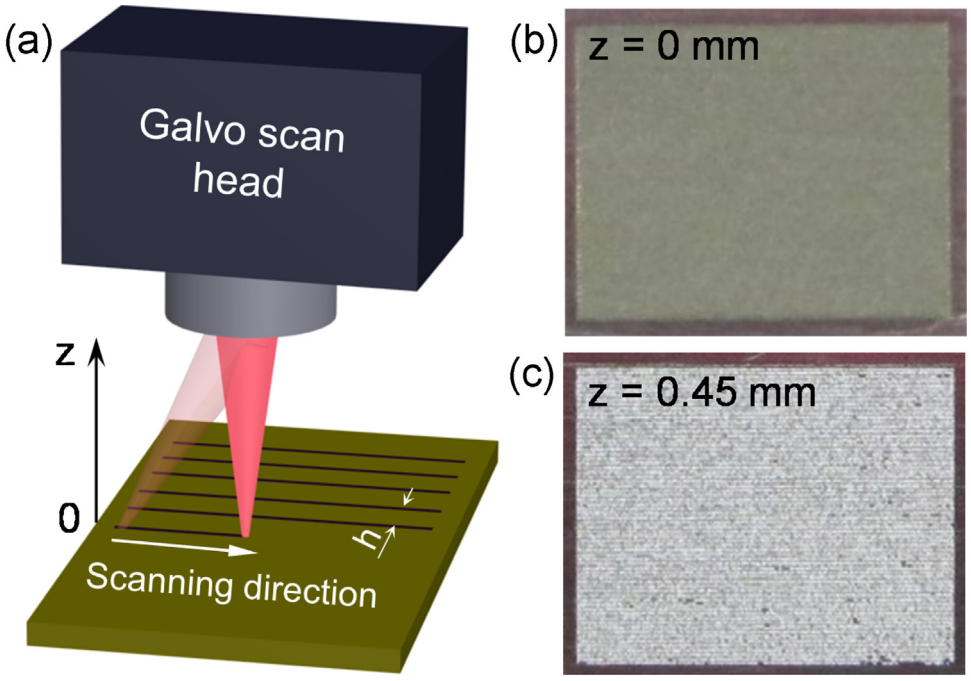

Fig. 2. Schematic of fabrication process and optical images of laser textured surfaces. (a) The scan head delivers the laser beam over the sample surface to generate microstructures. (b, c) sample images (7 mm × 6 mm), h = 75 μm, fabricated when z = 0 and 0.45 mm, respectively.

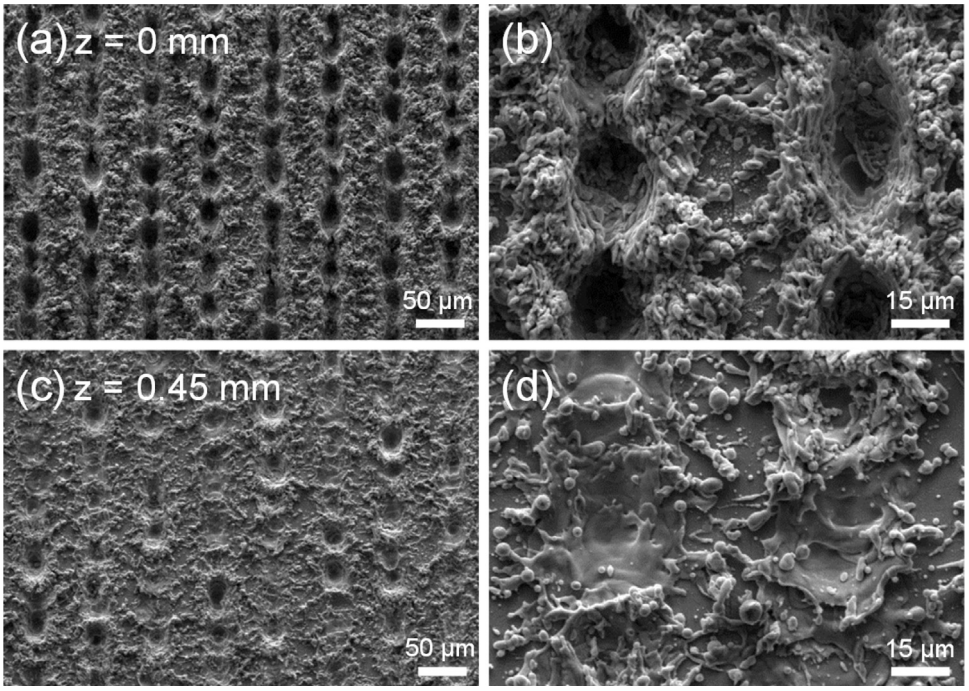

Fig. 3. Low and high magnification scanning electron microscope (SEM) images of the laser textured surfaces with h = 75 μm. (a, b) z = 0 mm. (c, d) z = 0.45 mm.

3.3. Time dependence of surface wettability

Directly after fabrication, both surfaces (z = 0 and 0.45 mm) exhibit a hydrophilic property characterized by small contact angle (<20°) compared with ~70° of the as-received surface. The contact angle of unprocessed surfaces does not show a significant change with time when exposed to ambient conditions (temperature of ~22 °C and relative humidity of ~44%). However, under the same environment, the contact angle for laser processed samples increased with time (Fig. 4). The contact angle development was faster for the samples fabricated with z = 0.45 mm compared with those created with z = 0 mm. For example, at day 4, the contact angles were 99° and 49°, for z = 0.45 and 0 mm respectively, a difference of 50°. However, it was observed that the difference in contact angle between the two surfaces becomes smaller with time. At 14 days, the difference is only 10° (151° and 141°). From 16 days, both surfaces exhibit superhydrophobic behaviour with similar and stable contact angles of ~154°. The result indicates that under the same conditions, the evolution of contact angle is faster for samples fabricated using a lower fluence, which is consistent with previous

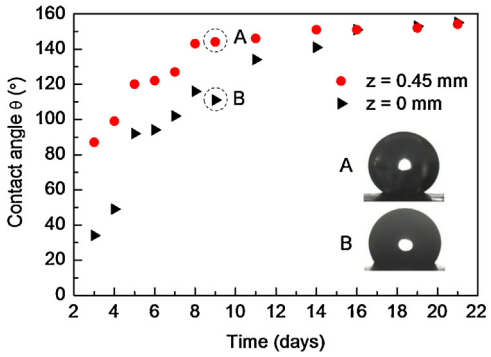

Fig. 4. Surface wettability evolution, characterized by the contact angle of textured samples over time, $h = 75\ \mu m$, processed with the defocus distance $z = 0$ and 0.45 mm. Each data point presented is an average value of two individual measurements. The inset shows droplet images on samples after exposure to air for 9 days.

reports on femtosecond laser patterned stainless steel [31]. Furthermore, the difference in contact angle between the two surfaces suggests that a wettability gradient is achievable from samples with roughness gradients.

The development of contact angle from hydrophobic to superhydrophobic on laser textured metallic surfaces has been previously reported and the mechanism is ascribed to modification of surface chemistry [31]. The observation of small contact angle directly after fabrication can be primarily explained by the surface morphology described by Wenzel equation [35]:

$$cos\theta_W = rcos\theta_f \quad (1)$$

where $r > 1$ is the roughness factor. θ_W and θ_f are contact angles on rough and flat surfaces, respectively. Accordingly to Eq. (1), roughness enhances the hydrophilic property of the surface and the higher the rough factor, the lower the contact angle. The change in wettability is, however, due to surface chemistry as there is no change in surface morphology with time. Indeed, from Eq. (1), it suggests that surface chemistry, which induces change in θ_f ($\Delta\theta_f$),would contribute to a comparative variation in θ_W ($\Delta\theta_W$)as following [36]:

$$\Delta\theta_W = r\left(\sin\theta_f/\sin\theta_W\right)\Delta\theta_f \quad (2)$$

In this work, it is believed that the adsorption of organic matter from the atmosphere [37] and partial deoxidation of copper oxide ($2CuO = Cu_2O + 1/2O_2$) [38] are two mechanism that were responsible for the change of surface wettability.

3.4. Surface morphology gradients

Fig. 5a illustrates a schematic for the fabrication of roughness gradients on a brass surface. The sample is tilted at an angle of α with one end located at the focal plane. As a result, the laser spot diameter, and thus laser fluence, gradually changes across the sample during the scanning process resulting in structure gradients. Fig. 5b shows an optical image of a typical fabricated surface gradient fabricated with $\alpha = 1.3°$. The sample exhibits a colour gradient from dark yellow (zone 1, high fluence) to light yellow (zone 3, low fluence). The surface morphology across the sample was studied. Fig. 5c shows the average surface roughness of samples created with $\alpha = 1.1°$ and 1.3°. Gradual variations of R_s from zone 1 to zone 3 can be seen for both cases. At zone 1, R_s was about 2.7 μm for both tilted angles. These values decreased to 1.8 μm for $\alpha = 1.1°$ and 1.5 μm for $\alpha = 1.3°$. To get a better vision of the surface morphology, SEM analysis was carried out on a sample created with $\alpha = 1.3°$ and the results are shown in Fig. 5d–f. The depth of the fabricated microgrooves decreases from zone 1 to zone 3. It is expected that other approaches such as a gradient filter can be used to control the laser power and surface roughness gradients can be obtained by directly writing laser on flat (instead of inclined) surfaces.

3.5. Surface wettability gradients

It has been shown surface morphology gradients on a brass surface can be obtained by laser writing. The surface roughness of these samples is no longer homogenous but a function of the coordinates $r(x,y)$, and therefore, the Wenzel equation is expressed in a general form [39]:

$$cos\theta_W = r(x,y)\,cos\theta_f \quad (3)$$

According to Eq. (3), a gradient of roughness would lead to a gradient of contact angle or wettability. Fig. 6 presents droplet images on three different zones (two edges and middle) of gradient surfaces created with $\alpha_1 = 1.3°$ after exposure to air for different time. At day 5 (Fig. 6a), the surface shows a wettability from hydrophilicity (zone 1, $\theta \sim 40°$) to hydrophobicity (zone 3, $\theta \sim 100°$). Contact angle across the surface increased with time, but the rate was different. After nine days, the contact angle was around 105° (zone 1), 125° (zone 2), and 140° (zone 3). That means the contact angle gap reduced from about 60 to 35° after four days.

Fig. 7 plots complete contact angle on surfaces fabricated with $\alpha = 1.1°$ and 1.3° versus time. It can be classified in two periods of time, before and after 17 days. Before 17 days, the surface exhibited a wettability gradient. For 1.3°, the variation of roughness is higher so there was a clear separation in contact angle among three zones, in which the contact angle at zone 3 was the highest, and as expected, the lowest at zone 1. For 1.1°, the contact angle at zone 3 was still the highest but the lowest measured angle fluctuated between zone 1 and 2 because of their small roughness differences. From 17 days, both surfaces became superhydrophobic with a contact angle of 150–154°. Hence, for some applications, the gradient surfaces may need to be temporally independent. It has been demonstrated that storing environments can strongly suppress the change of surface wettability [37], which is of interest for future investigations. Another possibility of freezing these gradients might be coating by a silanization layer [29]. However, simply immersing in boiling water to deactivate the active sites, as previously reported [31], would not work for these substrates as the surface will lose the hydrophobic property.

3.6. Application of surface gradients as multi-sensitivity chemical sensors

Responsive surfaces based on wettability have potential applications in microfluidics, smart devices and analysis of chemical solutions [40]. For surface gradients, the wettability responses to external environment is spatially dependent [12]. In this work, a chemical solvent (isopropanol) was used as a stimulus. Fig. 8 demonstrates that the contact angle of isopropanol solutions on the surface gradients decay exponentially with concentration. The effect is spatially dependent. A higher roughness leads to a lower decrease in contact angle and older samples are less responsive.

It is well-known that surface tension has an impact on the contact angle [41]. The contact angle of chemical solvents such as methanol and isopropanol was found to be very small, close to zero, on the laser processed surfaces. The contact angle for water on such a surface is high (~150° for those had been exposed to the air for 17 days or longer time). It therefore follows that the contact angle for a liquid which is a mixture of these solvents with water should depend on the concentration of the solvent. Furthermore, the contact angle also depends on surface properties. According to Eq. (1), it is proposed that the decrease of contact angle on rough surfaces is higher than that on flat surfaces, as it is amplified by roughness factor. Fig. 8a shows that the contact angle on an unprocessed

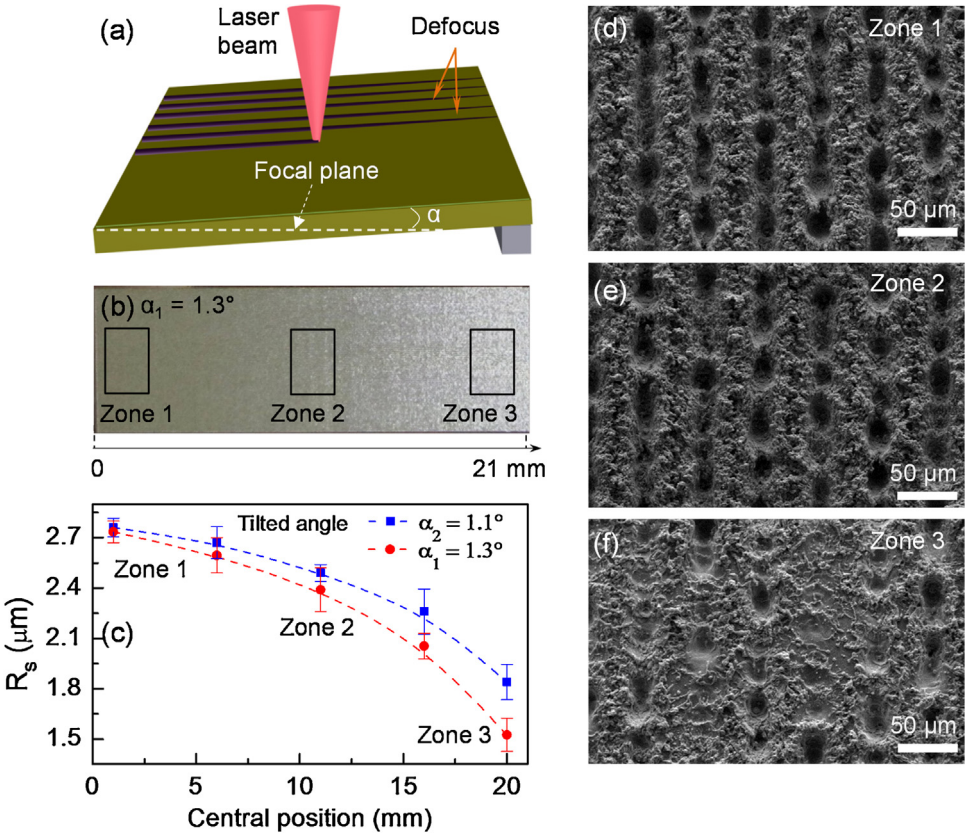

Fig. 5. (a) Schematic of surface gradients fabrication. Two tilted angles (α_1, α_2) are considered, 1.3° (α_1) and 1.1° (α_2). (b) Optical image of a surface gradient (7 mm × 21 mm, h = 50 μm) exhibits a colour gradient from zone 1 to zone 3. (c) Arithmetic average of surface roughness (R_s) across the gradient samples. (d)–(f) SEM images obtained on three different zones of the gradient sample fabricated when α_1 = 1.3°.

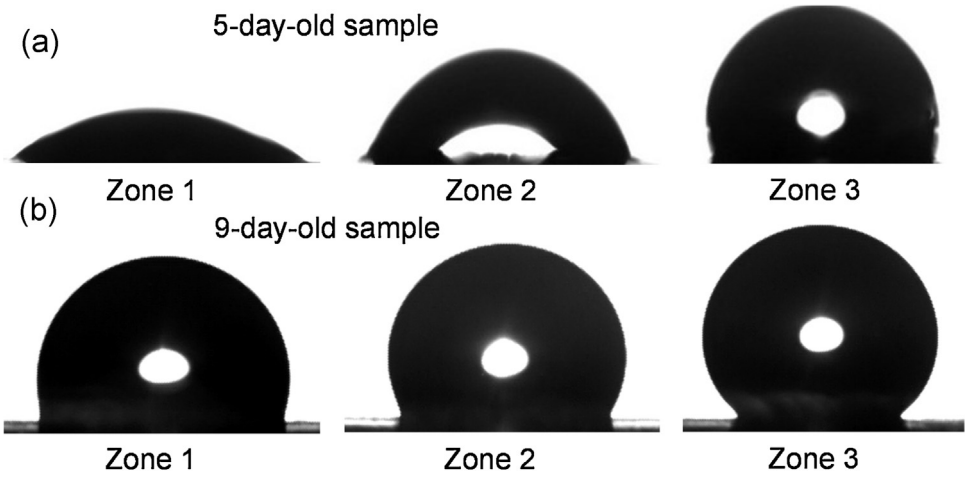

Fig. 6. Behaviour of water droplets on gradient surfaces at three different zones. Samples fabricated with α_1 = 1.3°, h = 50 μm and has been exposed to air for (a) 5 and (b) 9 days.

surface (the least roughness) reduced only 14°, from 69° to 55°, when the isopropanol concentration increases from 0 to 15.6 wt%. For surface gradient (29-day old), the contact angle dropped 84° (from 153° to 69°) at zone 3 and 132° (from 153° to 21°) at zone 1. That means at zone 1 (the highest roughness), the contact angle reduction is one order of magnitude higher compared with that of as-received surface. The decrease of contact angle with concentration is well described by an exponential decay function, which suggests that the surfaces can be used as solvent responsive devices or sensors. It has been shown that the contact angle change is spatially dependent so these so sensors based on such surfaces could have multi-sensitivity. Using both zone 1 and 3 in order to determine the concentration of an isopropanol solution would increase the accuracy.

Fig. 8b shows that the surfaces become less responsive when exposed to air for a longer period of time. For a sample that was 39 days old, the contact angle decreased from 154° to 40° at zone 1 and from 154° to 78° at zone 3. Compared with the 29 days old sample, the sensitivity has reduced about 10–14%. This is believed to be due to further surface chemistry modification. The result advises

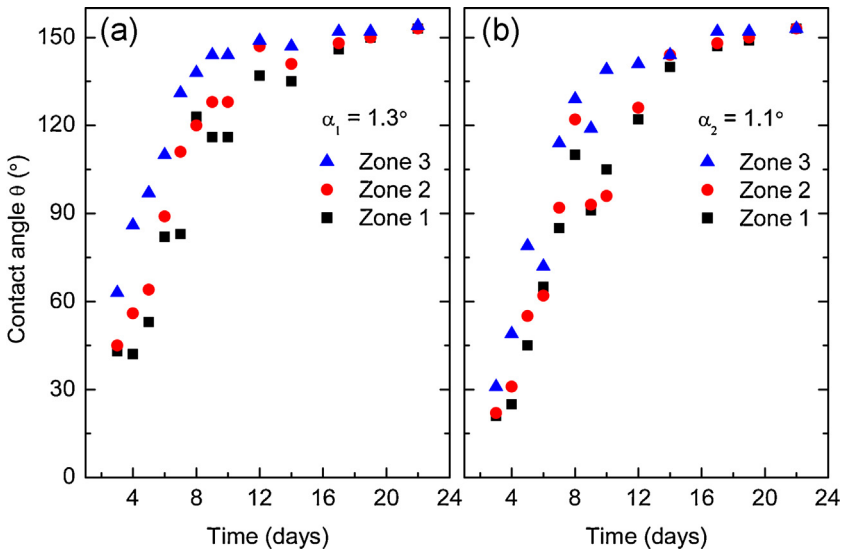

Fig. 7. Contact angle of water droplets measured over time on the surface gradients at three different zones. (a, b) The samples were processed with $h = 50\ \mu m$ and tilted angle of 1.3° and 1.1°, respectively. Each data point presented is an average value of two individual measurements.

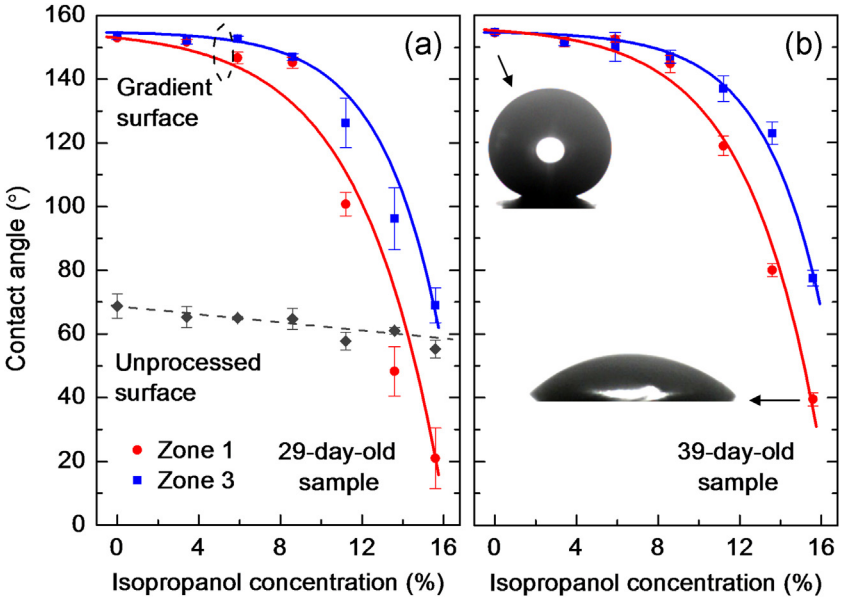

Fig. 8. Contact angle of isopropanol/water solution on the unprocessed as-received brass surface and laser textured gradient surfaces, $\alpha_1 = 1.3°$, $h = 50\ \mu m$. The samples were left under ambient conditions for (a) 29 and (b) 39 days after fabrication.

that an aging factor should be considered when using the surfaces for sensing applications. In addition, it is expected these surface sensors can be applied for sensing concentration of various organic solvents such as methanol, ethanol and acetone. The effect may also work for other water soluble chemical.

4. Conclusions

It has been demonstrated that surfaces with roughness gradients, and consequently wettability gradients, can be fabricated by direct laser texturing. The wettability is both spatially and temporally dependent, which is interesting for sensing applications. Proof-of-concept chemical sensors based on reduction of the contact angle with increased concentration are shown. In particular, the contact angle of isopropanol solution decays exponentially with concentration. The effect is spatially dependent. Areas with higher roughness exhibit higher contact angle decrease. That means different locations on the surface can be used as multi-channels for accurate measurement of the concentration. A decrease of 132° in contact angle on a surface gradient when isopropanol concentration is increased from 0 to 15.6 wt% has been observed. It is much more sensitive compared to 14° for unprocessed surfaces. This work provides a novel fabrication technology using low-waste and cost-effective nanosecond laser systems and a sensing principle for practical development of chemical sensors and smart surfaces.

Data availability

All relevant data present in this publication can be accessed at: http://dx.doi.org/10.17861/107b3672-3ced-428e-9f4c-b4e4bdc7c03c.

Acknowledgements

We thank Dr. Jim Buckman for helping with SEM measurements. This work is funded by the UK Engineering and Physical Sciences Research Council under grants EP/L017431/1, EP/L017350/1, EP/L016907/1 and EP/L017415/1.

References

[1] X. Zhang, F. Shi, J. Niu, Y. Jiang, Z. Wang, Superhydrophobic surfaces: from structural control to functional application, J. Mater. Chem. 18 (2008) 621–633.
[2] B. Bhushan, Y.C. Jung, Natural and biomimetic artificial surfaces for superhydrophobicity self-cleaning, low adhesion, and drag reduction, Prog. Mater. Sci. 56 (2011) 1–108.
[3] J. Drelich, E. Chibowski, D.D. Meng, K. Terpilowski, Hydrophilic and superhydrophilic surfaces and materials, Soft Matter 7 (2011) 9804–9828.
[4] F. Lugli, G. Fioravanti, D. Pattini, L. Pasquali, M. Montecchi, D. Gentili, M. Murgia, Z. Hemmatian, M. Cavallini, F. Zerbetto, And yet it moves! microfluidics without channels and troughs, Adv. Funct. Mater. 23 (2013) 5543–5549.
[5] J. Genzer, R.R. Bhat, Surface-bound soft matter gradients, Langmuir 24 (2008) 2294–2317.
[6] V.D. Ta, A. Dunn, T.J. Wasley, J. Li, R.W. Kay, J. Stringer, P.J. Smith, C. Connaughton, J.D. Shephard, Laser textured superhydrophobic surfaces and their applications for homogeneous spot deposition, Appl. Surf. Sci. 365 (2016) 153–159.
[7] Y.M. Zheng, H. Bai, Z.B. Huang, X.L. Tian, F.Q. Nie, Y. Zhao, J. Zhai, L. Jiang, Directional water collection on wetted spider silk, Nature 463 (2010) 640–643.
[8] J. Ju, H. Bai, Y.M. Zheng, T.Y. Zhao, R.C. Fang, L. Jiang, A multi-structural and multi-functional integrated fog collection system in cactus, Nat. Commun. 3 (2012) 1247, http://dx.doi.org/10.1038/ncomms2253.
[9] M.K. Chaudhury, G.M. Whitesides, How to make water run uphill, Science 256 (1992) 1539–1541.
[10] B.S. Gallardo, V.K. Gupta, F.D. Eagerton, L.I. Jong, V.S. Craig, R.R. Shah, N.L. Abbott, Electrochemical principles for active control of liquids on submillimeter scales, Science 283 (1999) 57–60.
[11] K. Ichimura, S.-K. Oh, M. Nakagawa, Light-driven motion of liquids on a photoresponsive surface, Science 288 (2000) 1624–1626.
[12] L. Ionov, N. Houbenov, A. Sidorenko, M. Stamm, I. Luzinov, S. Minko, Inverse and reversible switching gradient surfaces from mixed polyelectrolyte brushes, Langmuir 20 (2004) 9916–9919.
[13] Y. Einaga, G.-S. Kim, K. Ohnishi, S.-G. Park, A. Fujishima, Preparation of graded-morphology diamond thin films, Mater. Sci. Eng. B 83 (2001) 19–23.
[14] T.P. Kunzler, T. Drobek, C.M. Sprecher, M. Schuler, N.D. Spencer, Fabrication of material-independent morphology gradients for high-throughput applications, Appl. Surf. Sci. 253 (2006) 2148–2153.
[15] M. Reyssat, F. Pardo, D. Quéré, Drops onto gradients of texture, Europhys. Lett. 87 (2009) 36003.
[16] O. Bliznyuk, H.P. Jansen, E.S. Kooij, H.J.W. Zandvliet, B. Poelsema, Smart design of stripe-patterned gradient surfaces to control droplet motion, Langmuir 27 (2011) 11238–11245.
[17] S. Roy, N. Bhandaru, R. Das, G. Harikrishnan, R. Mukherjee, Thermally tailored gradient topography surface on elastomeric thin films, ACS Appl. Mater. Interfaces 6 (2014) 6579–6588.
[18] S. Daniel, M.K. Chaudhury, J.C. Chen, Fast drop movements resulting from the phase change on a gradient surface, Science 291 (2001) 633–636.
[19] S. Morgenthaler, S. Lee, S. Zürcher, N.D. Spencer, A simple, reproducible approach to the preparation of surface-chemical gradients, Langmuir 19 (2003) 10459–10462.
[20] X. Yu, Z. Wang, Y. Jiang, X. Zhang, Surface gradient material: from superhydrophobicity to superhydrophilicity, Langmuir 22 (2006) 4483–4486.
[21] N. Ballav, A. Shaporenko, A. Terfort, M. Zharnikov, A flexible approach to the fabrication of chemical gradients, Adv. Mater. 19 (2007) 998–1000.
[22] D.J. Huang, T.S. Leu, Fabrication of high wettability gradient on copper substrate, Appl. Surf. Sci. 280 (2013) 25–32.
[23] G.Y. Zhang, X. Zhang, M. Li, Z.H. Su, A surface with superoleophilic-to-superoleophobic wettability gradient, ACS Appl. Mater. Interfaces 6 (2014) 1729–1733.
[24] G. Fioravanti, F. Lugli, D. Gentili, V. Mucciante, F. Leonardi, L. Pasquali, A. Liscio, M. Murgia, F. Zerbetto, M. Cavallini, Electrochemical fabrication of surface chemical gradients in thiol self-assembled mono layers with tailored work-functions, Langmuir 30 (2014) 11591–11598.
[25] T.H. Her, R.J. Finlay, C. Wu, S. Deliwala, E. Mazur, Microstructuring of silicon with femtosecond laser pulses, Appl. Phys. Lett. 73 (1998) 1673–1675.
[26] A.Y. Vorobyev, C.L. Guo, Direct femtosecond laser surface nano/microstructuring and its applications, Laser Photon. Rev. 7 (2013) 385–407.
[27] A. Dunn, J.V. Carstensen, K.L. Wlodarczyk, E.B. Hansen, J. Gabzdyl, P.M. Harrison, J.D. Shephard, D.P. Hand, Nanosecond laser texturing for high friction applications, Opt. Lasers Eng. 62 (2014) 9–16.
[28] A.M. Kietzig, M.N. Mirvakili, S. Kamal, P. Englezos, S.G. Hatzikiriakos, Laser-patterned super-hydrophobic pure metallic substrates: Cassie to Wenzel wetting transitions, J. Adhes. Sci. Technol. 25 (2011) 2789–2809.
[29] S. Moradi, S. Kamal, P. Englezos, S.G. Hatzikiriakos, Femtosecond laser irradiation of metallic surfaces: effects of laser parameters on superhydrophobicity, Nanotechnology 24 (2013) 415302.
[30] M.V. Rukosuyev, J. Lee, S.J. Cho, G. Lim, M.B.G. Jun, One-step fabrication of superhydrophobic hierarchical structures by femtosecond laser ablation, Appl. Surf. Sci. 313 (2014) 411–417.
[31] A.-M. Kietzig, S.G. Hatzikiriakos, P. Englezos, Patterned superhydrophobic metallic surfaces, Langmuir 25 (2009) 4821–4827.
[32] D.V. Ta, A. Dunn, T.J. Wasley, R.W. Kay, J. Stringer, P.J. Smith, C. Connaughton, J.D. Shephard, Nanosecond laser textured superhydrophobic metallic surfaces and their chemical sensing applications, Appl. Surf. Sci. 357 (2015) 248–254.
[33] C. Sun, X.W. Zhao, Y.H. Han, Z.Z. Gu, Control of water droplet motion by alteration of roughness gradient on silicon wafer by laser surface treatment, Thin Solid Films 516 (2008) 4059–4063.
[34] A.D. Sommers, T.J. Brest, K.F. Eid, Topography-based surface tension gradients to facilitate water droplet movement on laser-etched copper substrates, Langmuir 29 (2013) 12043–12050.
[35] R.N. Wenzel, Resistance of solid surfaces to wetting by water, Ind. Eng. Chem. 28 (1936) 988–994.
[36] G. McHale, N.J. Shirtcliffe, M.I. Newton, Super-hydrophobic and super-wetting surfaces: analytical potential? Analyst 129 (2004) 284–287.
[37] J. Long, M. Zhong, P. Fan, D. Gong, H. Zhang, Wettability conversion of ultrafast laser structured copper surface, J. Laser Appl. 27 (2015) S29107.
[38] F.-M. Chang, S.-L. Cheng, S.-J. Hong, Y.-J. Sheng, H.-K. Tsao, Superhydrophilicity to superhydrophobicity transition of CuO nanowire films, Appl. Phys. Lett. 96 (2010) 114101.
[39] M. Nosonovsky, On the range of applicability of the Wenzel and Cassie equations, Langmuir 23 (2007) 9919–9920.
[40] B.W. Xin, J.C. Hao, Reversibly switchable wettability, Chem. Soc. Rev. 39 (2010) 769–782.
[41] W. Choi, A. Tuteja, S. Chhatre, J.M. Mabry, R.E. Cohen, G.H. McKinley, Fabrics with tunable oleophobicity, Adv. Mater. 21 (2009) 2190–2195.